The Impact of Transmission Line Modeling on Lightning Performance of Line Surge Arresters - Part II: Impact on the Power and Energy Dissipation ⋆

Jaimis S. L. Colqui * **Rodolfo A. R. Moura** **
Marco Aurélio O. Schroeder ** **José Pissolato Filho** *

* *School of Electrical and Computer Engineering, State University of Campinas, Brazil (e-mail: jaimis@unicamp.br; pisso@unicamp.br)*
** *Electrical Engineering Department, Federal University of São João del-Rei, Brazil (e-mail: moura@ufsj.edu.br; schroeder@ufsj.edu.br)*

Abstract: This paper investigates the impact of the transmission line parameter calculation formulations in the evaluation of power and energy dissipated in line surge arresters. The results are achieved by simulations in ATP software, considering typical Brazilian conditions of transmission lines. The calculation of the line parameters is computed in three ways, namely: i) Carson' formulation, ii) Nakagawa's formulation considering the ground parameters constant with frequency, and ii) Nakagawa's formulation considering the frequency-dependent characteristics of soil. Taking as reference the results determined by Carson's formulation (since this formulation is the most used in programs for calculating transients), it is shown that Nakagawa's formulations considering both constant and frequency-dependent soil parameters can lead to differences in energy dissipated in surge arresters in transmission lines partially or totally protected by surge arresters. According to the results, depending on the case, maximum differences in power and energies of up to 10.547% and 11.76%, respectively, can be found.

Keywords: Transmission line modeling; surge arresters; lightning protection; frequency dependent behaviour; grounding; time-domain simulations.

1. INTRODUCTION

Part I of this paper (Colqui et al., 2022) investigates the impact of representation of the different models for calculating transmission line (TL) parameters in computer simulations in the performance of lightning surge arrester (SA) of TL. According to results, the phases in which it is not considered the SA, the overvoltages differences are up to 4.30%. On the other hand, in phases protected by surge arresters, the differences observed in the waveforms for the three representations are up to 6.42%.

However, other utmost importance in SA design are the power and energy dissipated by the lightning arresters. Thus, part II of this work aims to evaluate the influence of the representation of the different models for calculating line parameters on the results of simulations of the power and energy absorbed by SA. As in the part I of this work, results are presented for three formulations for calculating line parameters and conditions contemplating lines partially protected (lightning arresters in one or two phases) and completely protected (lightning arresters in all phases), and the soil resistivities of 1,000 Ω. m, 3,000 Ω.m and 10,000 Ω.m. These formulations are: i) Carson formulation, ii) Nakagawa formulation considering the ground parameters constant with frequency, and ii) Nakagawa formulation considering the frequency-dependent characteristics of soil.

The paper is organized as follows: Section 2 presents the models used to simulate the electromagnetic transients in the software Alternative Transients Program (ATP). Section 3 presents the methodology used to set the SA. Section 4 is devoted to present the dissipated energy impact considering models that calculate the TL parameters. The main conclusions of this paper are presented in Section 5.

2. MODELING

As in Part I, the results are obtained from time domain simulations of TLs partially and totally protected by lightning arresters subjected to lightning currents at the top of their towers. Conditions typically observed in Brazilian TLs are simulated. The models adopted for the simulations carried out in this Part II are the same previously adopted, and described in detail, in Part I. To model the tower foot grounding system, the rigorous Hybrid Electromagnetic Model (HEM) (Visacro and Soares, 2005) is used in the frequency domain and included in the time domain simulations by an equivalent circuit synthesized using the Vector Fitting method (Gustavsen, 2008, 2022). Furthermore, the simulations were performed under the assumption of frequency-dependent electrical parameters, considering a rigorous causal model (Alípio and Visacro, 2014).

⋆ This work was supported by São Paulo Research Foundation (FAPESP) (grant: 2021/06157-5).

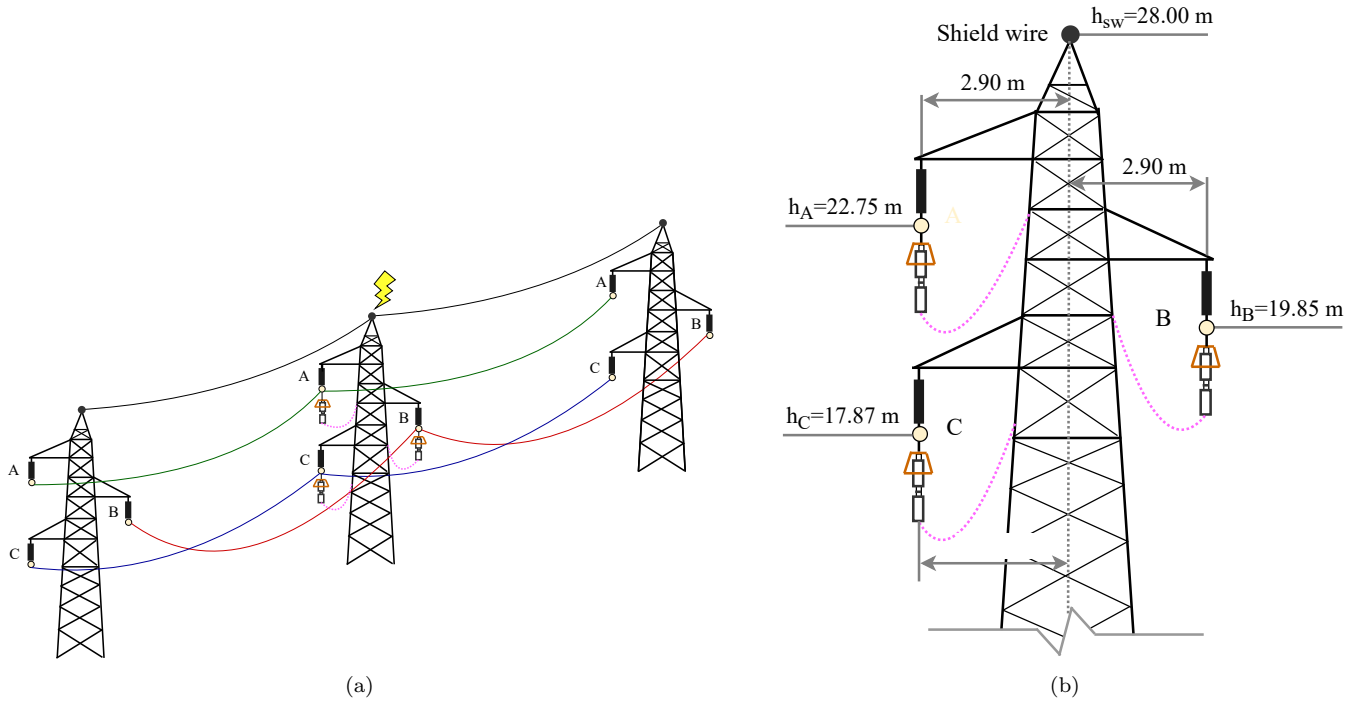

Figure 1. Configuration of the 138-kV analyzed in the present paper.

The towers are modeled using a system of vertical multi-conductors, with each conductor represented by a single-phase lossless line (De Conti et al., 2006). The SA are represented by the dynamic model of metallic zinc oxide SA proposed by IEEE (1992). The lightning current is represented by the wave proposed in the CIGRE Brochure (CIGRE Working Group C4.23, 2021), which contemplates the concave nature of the first return strokes, as well as the occurrence of the maximum derivative near the peak (De Conti and Visacro, 2007).

Three models are adopted in this paper to represent the TL, as follows:

(1) The first model, the line model proposed by JMarti (Marti, 1982) which is the most popular model for the digital simulation of electromagnetic transients on TLs. The JMarti setup available in the LCC routine of ATPDraw considers Carson's formulation for calculating the parameters of lines (Marti, 1982). Among other aspects, Carson's formulation, displacement currents in soil are negligible in comparison with conductive currents. Furthermore, the frequency dependence of soil parameters is disregarded.

(2) A second model, here called modified Marti's model is used. The implementation of this modified model in ATP software was proposed in De Conti and Emídio (2016). The implementation of this model consists of writing in a .pch file the data related to the calculation of the line parameters (poles and residues of the propagation and impedance matrices characteristics are written, together with the minimum time delays and the real transformation matrix). This .pch file is interpreted in ATP software as a TL model of JMarti type (see De Conti and Emídio (2016) for details). To calculate the parameters of the line, the formulation that considers displacement currents, the Nakagawa formulation, was used, but we consider soil parameters constant with frequency.

(3) The third model is the same as the second model, but considering the frequency-dependence of the soil in Nakagawa's formulation.

In order to compare the aforementioned models os TLs, Table 1 summarizes three different representations, deliberately chosen, of the transmission system models. These representations were set to be used in the simulations. Also, the low-frequency soil resistivities considered are: 1,000 Ω.m., 3,000 Ω.m. and 10,000 Ω.m. For these resistivities, it was considered the effective length, obtained by using CIGRE Working Group C4.23 (2021). The effective length and low frequency resistance of the counterpoise cable are shown in Table 2.

For the SA model to compute the power and energy dissipated, the 11 towers and the 12 spans considered in part I and the lightning current striking at the top of the central tower were considered, as shown in Fig 1(a). The silhouette of the tower and the line cable heights are illustrated in Fig. 1(b), and the phase conductors and shield wire data were shown in part I.

Table 1. Types of modeling representations.

Rep.	TL model	Appro.	Soil for TL	Ground. model
1	JMarti	Carson	ρ_0	Z ($\rho(\omega)$, $\varepsilon_r(\omega)$)
2	Modified Marti's	Nakagawa	ρ_0, ε_r	Z ($\rho(\omega)$, $\varepsilon_r(\omega)$)
3	Modified Marti's	Nakagawa	$\rho(\omega)$, $\varepsilon_r(\omega)$	Z ($\rho(\omega)$, $\varepsilon_r(\omega)$)

Table 2. Length of the counterpoise wires as a function of soil resistivity.

ρ_0 [Ω.m]	1,000	3,000	10,000
L_{EF} [m]	55	100	180

3. SIMULATION METHODOLOGY

Differences in the powers and energies absorbed by the SA installed in the tower can be found depending on the representations of the TLs model, considering a TL protected with SA only in phase C, SA only in phases B and C and SA in phases A, B, and C. Moreover, this differences also occur depending on the soil resistivities. Hence, in this paper three soil resistivities were considered being 1,000 Ω.m, 3,000 Ω.m and 10,000 Ω.m. Lightning currents are considered with values corresponding to the median value determined from measurements of real discharges at the Morro do Cachimbo Station (Visacro et al., 2004).

All simulations were performed in ATP. The power and energy dissipated in the SA was determined from the product of voltage and current instantaneous power, and the integral of this product, respectively. This computation generates similar results when using the software tool for energy calculation (Power & Energy), applied to each energy dissipating element. The schematic representation of this systems is shown in Fig. 2.

4. RESULTS

This section presents simulation results of power and energy dissipated in SA installed in TL due to lightning incidence in the top of the tower. The main objective of this paper is to compare the power and the energy dissipated by the SA when using different formulations of calculate the TL model. An extensive set of simulations was carried out, contemplating partially protected lines (SA in one or in two phases) and fully protected (SA in all phases).

In the subsection 4.1, comparisons of the power dissipated by the SA installed in the transmission tower are shown. In the subsection 4.2, comparisons of the energies dissipated by the SA installed in the transmission tower are shown.

4.1 Surger Arrester Instantaneous Power

Figs. 3, 4 and 5 illustrates the power of SA installed only in phase C, only in phases B and C, and installed in phases A , B and C of the 138-kV line, respectively. In these figures, the three representations of the TL shown in Table 1 were considered, and the value of the soil resistivity, at

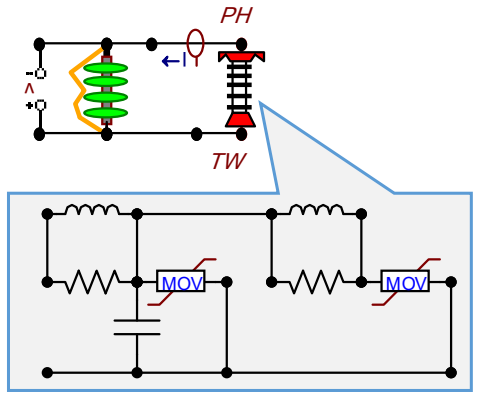

Figure 2. Mechanism for evaluating the power and energy absorbed in the lightning arrester from its representation in ATPDraw.

low frequency, of 1,000 Ω.m, 3,000 Ω.m and 10,000 Ω.m were considered.

In all the figures it can be seen that the power when considering SA in phase C, they are greater than if considering SA in phases B and C, and these are greater than if considering SA in phases A, B, and C. Likewise, it can be noted that the powers by the SA installed on the line when we consider a soil with a resistivity of 1,000 Ω.m, are smaller than we consider a soil with a resistivity of 3,000 Ω.m , and these are smaller than when we consider a soil with a resistivity of 10,000 Ω.m.

In the case of Fig. 3, it can be observed, for all TL representations and soil resistivities, differences in the peak values and along the curve. The biggest differences are between representation 3 and representation 1, when considering the resistivity of 10,000 Ω.m. This is because for the resistivity of 10,000 Ω.m the TL models Carson and Nakagawa do have much difference at high frequencies (Colqui et al., 2021).

Table 3, show the peaks of the power (from Fig. 3) for the three representations. The maximum differences of representations 2 and 3 in relation to representation 1 are also shown. The biggest difference found was 7.227% which corresponds to considering representation 3 and a soil of 10,000 Ω.m

In the case of Fig. 4, it can be observed for all TL representations and soil resistivities differences in the peak values and along the power curve. Also, at the peaks and maximum differences of the consumed power (from Fig. 4) for the three representations is shown in Table 4. The biggest difference found was 11.33% which corresponds when considering representation 3 and a soil of 10,000 Ω.m

In the case of Fig. 5, it can be observed for all TL representations and soil resistivities differences in the peak and along the power curve. Also, at the peaks and maximum differences of the power (from Fig. 5) for the three representations is shown in Table 5. The biggest difference

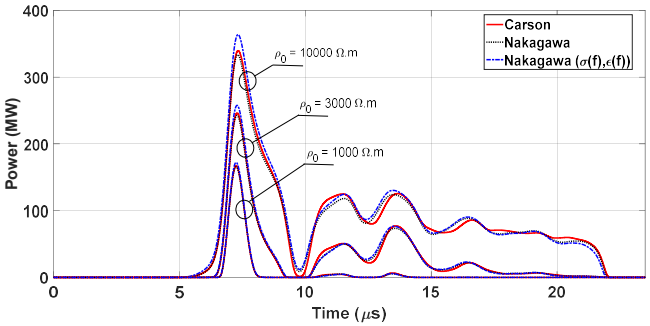

Figure 3. Power consumed by the TL surge arrester with only surge arrester in phase C.

Table 3. $P_{\max}$ and ΔP(%) obtained with only lightning arresters in phase C.

	$P_{\max}$ (MW)			ΔP(%)		
	ρ_0 (Ω.m)			ρ_0 (Ω.m)		
Rep.	1,000	3,000	10,000	1,000	3,000	10,000
1 (Phase C)	167.3	246.0	339.0	-	-	-
2 (Phase C)	165.6	242.4	333.1	1.016	1.463	1.741
3 (Phase C)	172.2	257.6	363.5	2.929	4.715	7.227

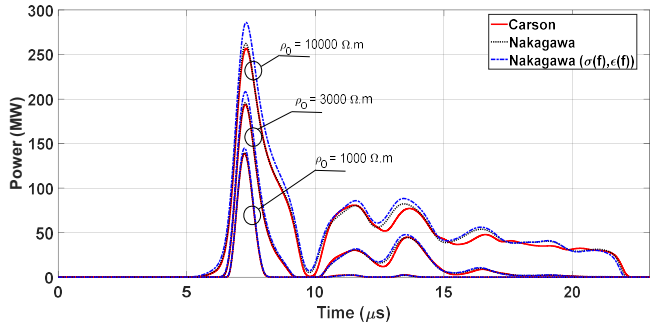

(a)

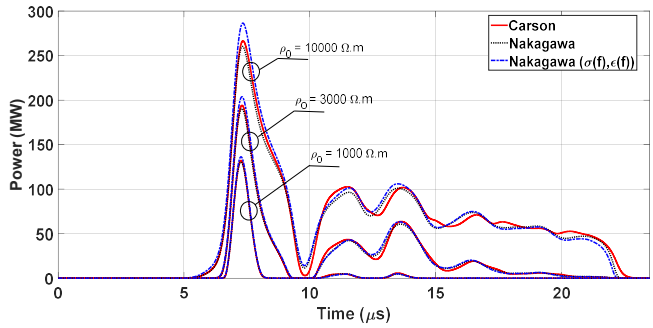

(b)

Figure 4. Power consumed by the TL surge arrester with only surge arrester in phases B and C; (a) Phase B and (b) Phase C.

Table 4. $P_{\max}$ and ΔP(%) obtained with only lightning arrester in phases B and C.

	$P_{\max}$ (MW)			ΔP(%)		
	ρ_0 (Ω.m)			ρ_0 (Ω.m)		
Rep.	1,000	3,000	10,000	1,000	3,000	10,000
1 (Phase B)	138.9	193.7	256.8	-	-	-
2 (Phase B)	139.4	195.8	262.3	0.360	1.084	2.141
3 (Phase B)	144.8	208.2	285.9	4.247	7.485	11.33
1 (Phase C)	132.2	194.0	266.1	-	-	-
2 (Phase C)	130.4	190.4	260.0	1.361	1.855	2.292
3 (Phase C)	136.3	203.6	286.2	3.101	4.948	7.553

found was 11.75% which corresponds when considering representation 3 and a soil of 10,000 Ω.m

4.2 Surger Arrester Energy Dissipation

Figs. 6, 7 and 8 illustrate the accumulated energies dissipated by SA for the same cases as in subsection 4.1. Similarly to the power cases, in all the figures it can be seen that the energies dissipated by the SA when considering SA in phase C, they are greater than if considering SA in phases B and C, and these are greater than if considering SA in phases A, B, and C. Likewise, it can be noted that the energies dissipated by the lightning arrester installed on the line when we consider a soil with a resistivity of 1,000 Ω.m, are smaller than we consider a soil with a resistivity of 3,000 Ω.m , and these are smaller than when we consider a soil with a resistivity of 10,000 Ω.m.

In the case of Fig. 6, it can be observed for all TL representations and soil resistivities differences in values along the accumulated energy curve. The biggest differences are between representation 3 and representation 1, when considering the resistivity of 10,000 Ω.m. As in the

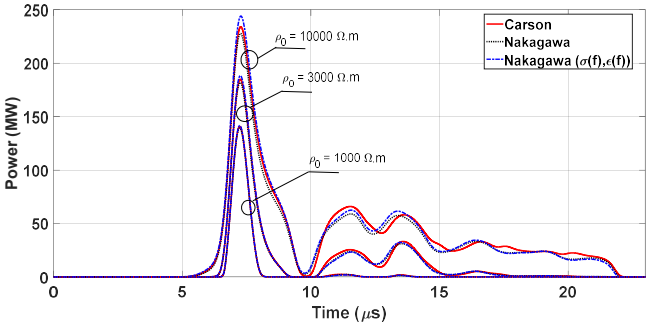

(a)

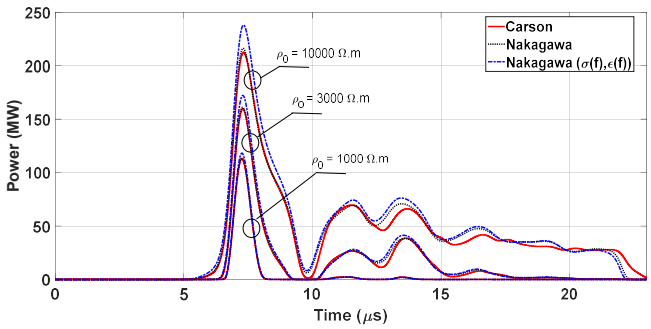

(b)

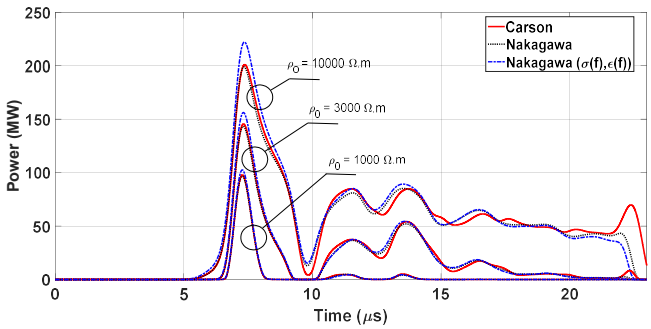

(c)

Figure 5. Power consumed by the TL surge arrester with surge arrester in phases A, B and C; (a) Phase A, (b) Phase B and (c) Phase C.

Table 5. $P_{\max}$ and ΔP(%) obtained with only lightning arrester in phases A, B and C.

	$P_{\max}$ (MW)			ΔP(%)		
	ρ_0 (Ω.m)			ρ_0 (Ω.m)		
Rep.	1,000	3,000	10,000	1,000	3,000	10,000
1 (Phase A)	140.8	184.8	234.0	-	-	-
2 (Phase A)	139.3	181.9	227.8	1.065	1.569	2.649
3 (Phase A)	141.6	188.3	244.1	0.568	1.893	4.316
1 (Phase B)	113.1	159.6	212.6	-	-	-
2 (Phase B)	113.4	161.1	216.2	0.265	0.939	1.693
3 (Phase B)	118.2	172.1	237.6	4.509	7.832	11.75
1 (Phase C)	97.79	145.3	201.0	-	-	-
2 (Phase C)	96.70	143.2	198.8	1.114	1.445	1.094
3 (Phase C)	102.5	156.1	222.2	4.816	7.432	10.547

power analysis, this is because for the resistivity of 10,000 Ω.m the TL models Carson and Nakagawa do have much difference at high frequencies (Colqui et al., 2021).

Table 6, show the dissipated energies (from Fig. 6) for the three representations. The maximum differences of representations 2 and 3 in relation to representation 1 are

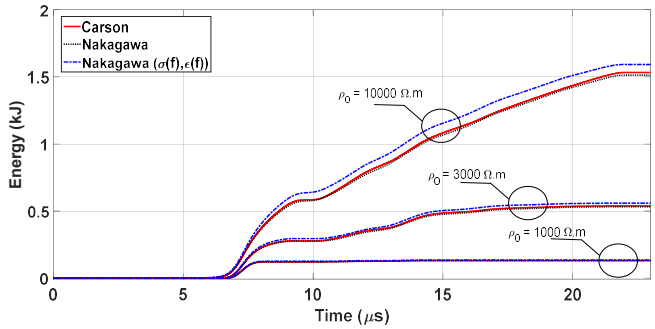

Figure 6. Energy dissipated by the TL with SA only in phase C.

Table 6. Dissipated Energy and ΔE(%) obtained considering only the lightning arrester in phase C.

	E_{max} (kJ)			ΔE(%)		
	ρ_0 (Ω.m)			ρ_0 (Ω.m)		
Rep.	1,000	3,000	10,000	1,000	3,000	10,000
1 (Phase C)	0.131	0.540	1.533	-	-	-
2 (Phase C)	1.129	0.532	1.513	1.144	1.481	1.305
3 (Phase C)	0.135	0.559	1.592	2.974	3.518	3.848

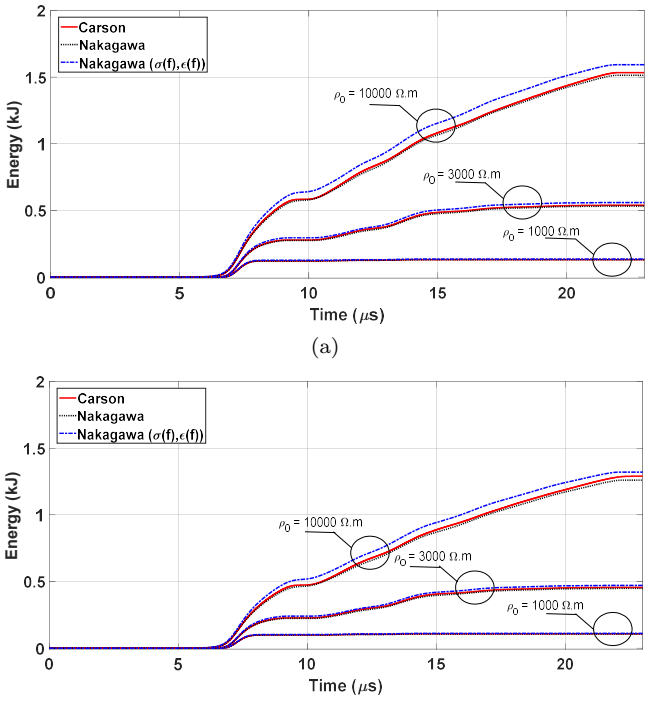

Figure 7. Energy dissipated by the TL with surge arrester only in phases B and C; (a) phase B, and (b) phase C.

also shown. The biggest difference found was 3.848% which corresponds to considering representation 3 and a soil of 10,000 Ω.m.

In the case of Fig. 7, it can be observed for all TL representations and soil resistivities differences in along the accumulate energy curve. The maximum difference between the three representations is shown in Table 7. The biggest difference found was 11.76% which corresponds

Table 7. Dissipated Energy and ΔE(%) obtained considering only the lightning arrester in phases B and C.

	E_{max} (kJ)			ΔE(%)		
	ρ_0 (Ω.m)			ρ_0 (Ω.m)		
Rep.	1,000	3,000	10,000	1,000	3,000	10,000
1 (Phase B)	0.104	0.339	0.968	-	-	-
2 (Phase B)	0.105	0.349	1.008	0.670	2.291	4.121
3 (Phase B)	0.109	0.372	1.082	5.172	9.564	11.76
1 (Phase C)	0.107	0.456	1.290	-	-	-
2 (Phase C)	0.106	0.4481	1.260	1.486	1.689	2.325
3 (Phase C)	0.111	0.471	1.321	2.973	3.247	2.403

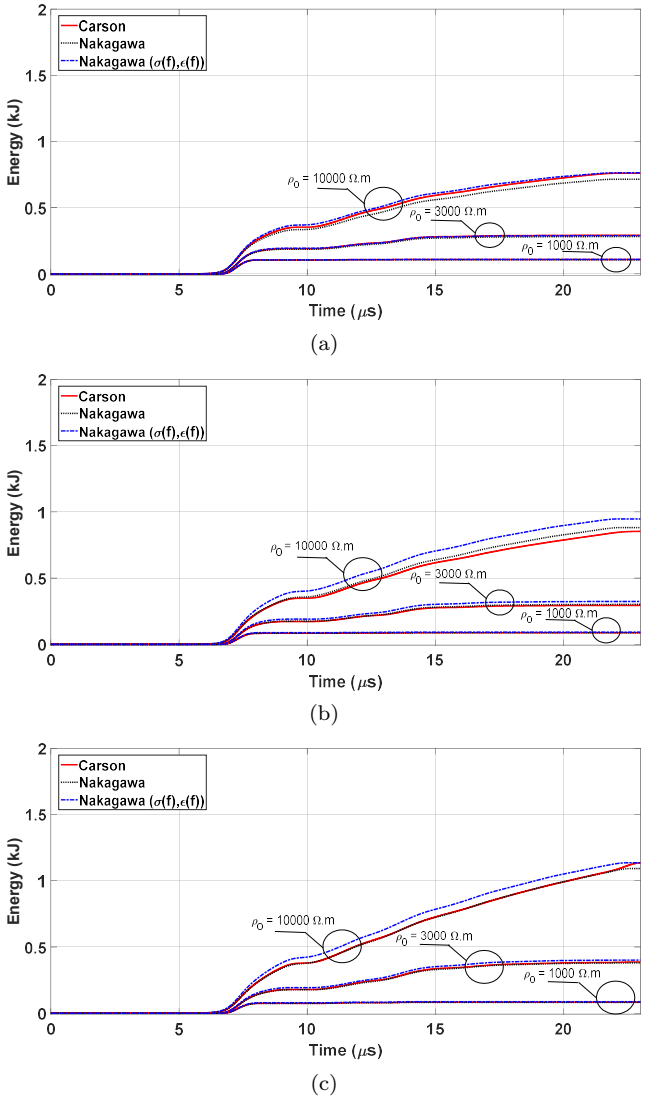

Figure 8. Energy dissipated by the TL with surge arrester in phases A, B and C; (a) phase A, (b) phase B and (c) phase C.

when considering representation 3 (phase B) and a soil of 10,000 Ω.m.

Finally, In the case of Fig. 8, it can be observed for all TL representations and soil resistivities differences in along the accumulate energy curve. The maximum difference between the three representations is shown in Table 8. The biggest difference found was 10.98% which corresponds

when considering representation 3 (phase B) and a soil of 10,000 Ω.m.

Table 8. Dissipated Energy and ΔE(%) obtained considering only the lightning arrester in phases A, B and C.

	E_{max} (kJ)			ΔE(%)		
	ρ_0 (Ω.m)			ρ_0 (Ω.m)		
Rep.	1,000	3,000	10,000	1,000	3,000	10,000
1 (Phase A)	0.109	0.291	0.761	-	-	-
2 (Phase A)	0.107	0.282	0.715	1.735	3.359	5.920
3 (Phase A)	0.110	0.289	0.763	0.091	0.719	0.381
1 (Phase B)	0.086	0.293	0.853	-	-	-
2 (Phase B)	0.087	0.301	0.882	0.518	2.587	3.329
3 (Phase B)	0.097	0.323	0.947	5.447	10.11	10.98
1 (Phase C)	0.083	0.387	1.136	-	-	-
2 (Phase C)	0.084	0.380	1.092	0.876	1.884	3.873
3 (Phase C)	0.086	0.401	1.135	4.275	3.510	0.088

5. CONCLUSIONS

The present study evaluated differences in the simulated behavior of lightning arresters from different representations of the transmission line model, considering the formulations of Carson, Nakagawa with ground parameters constant with frequency and with ground parameters variable with frequency. According to results, the behavior of surge arresters from the point of view of power consumption and energy absorption is also impacted up to 10.547% and 11.76%, respectively, by the formulation adopted for the transmission line model.

These differences are justified by the different behavior of the transmission line parameter calculation formulations against high frequency currents. As lightning strikes have a wide spectrum of frequencies, from 0 Hz to a few MHz, these differences reflect on a behavior of the transmission line model, which in turn interferes with the overvoltage values reached in insulator strings, power and energy dissipation in SA.

The simulations carried out in Parts I and II of this work also showed that the representation of the calculation of transmission line parameters from its behavior represented by Carson's formulation incurs not so considerable errors, compared to its rigorous behavior (formulation of Nakagawa which includes frequency-dependent soil parameters) against lightning strikes. On the other hand, these errors present a conservative approach on the behavior of lightning arresters applied to transmission lines, both from the point of view of overvoltages in unprotected phases, as well as the power and energy. It is also noted that the values of total energy dissipated are higher the more unfavorable the grounding conditions of the transmission tower are, i.e., the higher the soil resistivity the higher is the energy.

REFERENCES

Alípio, R.S. and Visacro, S. (2014). Modeling the frequency dependence of electrical parameters of soil. *IEEE Transactions on Electromagnetic Compatibility*, 56(5), 1163–1171.

CIGRE Working Group C4.23 (2021). Procedures for Estimating the Lightning Performance of Transmission Lines – New Aspects.

Colqui, J.S.L., Araújo, A.R.J., Pascoalato, T.F.G., and Kurokawa, S. (2021). Transient analysis of overhead transmission lines based on fitting methods. In *2021 14th IEEE International Conference on Industry Applications (INDUSCON)*, 180–187.

Colqui, J.S.L., Moura, R.A., Schroeder, M.A.O., and Filho, J.P. (2022). The Impact of Transmission Line Modeling on Lightning Performance of Line Surge Arresters - Part I: Impact on the Overvoltages. *XXIV Brazilian Congress of Automatics (CBA)*.

De Conti, A. and Emídio, M.P.S. (2016). Extension of a modal-domain transmission line model to include frequency-dependent ground parameters. *Electric Power Systems Research*, 138, 120–130.

De Conti, A. and Visacro, S. (2007). Analytical representation of single- and double-peaked lightning current waveforms. *IEEE Transactions on Electromagnetic Compatibility*, 49(2), 448–451.

De Conti, A., Visacro, S., Soares, A., and Schroeder, M.A.O. (2006). Revision, extension, and validation of Jordan's formula to calculate the surge impedance of vertical conductors. *IEEE Transactions on Electromagnetic Compatibility*, 48(3), 530–536.

Gustavsen, B. (2008). *User's Guide for vectfit3.m (Fast Relaxed Vector Fitting)*. SINTEF Energy Research, N-7465 Trondheim, Norway.

Gustavsen, B. (2022). URL `https://www.sintef.no/projectweb/vectorfitting/`. Matrix Fitting Toolbox.

IEEE (1992). *Working Group on Surge Arrester*, Modeling of Metal Oxide Surge Arresters. *IEEE Transactions on Power Delivery*, 7(1), 302–309.

Marti, J.R. (1982). Accurate Modeling of Frequency-Dependent Transmission Lines in Electromagnetic Transient Simulations. *IEEE Power Engineering Review*, 2(1), 29–30.

Visacro, S. and Soares, A. (2005). HEM: A model for simulation of lightning-related engineering problems. *IEEE Transactions on Power Delivery*, 20(2 I), 1206–1208.

Visacro, S., Soares Jr, A., Schroeder, M.A.O., Cherchiglia, L.C., and de Sousa, V.J. (2004). Statistical analysis of lightning current parameters: Measurements at Morro do Cachimbo Station. *Journal of Geophysical Research*, 109(DO1105), 1–11.